Gamma-Ray and Neutron Spectrometer for the Dawn Mission to 1 Ceres and 4 Vesta

Thomas H. Prettyman, *Member, IEEE*, William C. Feldman, Frank P. Ameduri, Bruce L. Barraclough, Ethan W. Cascio, Kenneth R. Fuller, Herbert O. Funsten, *Member, IEEE*, David J. Lawrence, Gregg W. McKinney, Christopher T. Russell, Stephen A. Soldner, *Member, IEEE*, Steven A. Storms, Csaba Szeles, and Robert L. Tokar

***Abstract*—We present the design of the gamma-ray and neutron spectrometer (GR/NS) for Dawn, which is a NASA Discovery-class mission to explore two of the largest main-belt asteroids, 1 Ceres and 4 Vesta, whose accretion is believed to have been interrupted by the early formation of Jupiter. Dawn will determine the composition and structure of these protoplanetary bodies, providing context for a large number of primitive meteorites in our sample collection and a better understanding of processes occurring shortly after the onset of condensation of the solar nebula. The Dawn GR/NS design draws on experience from the successful Lunar Prospector and Mars Odyssey missions to enable accurate mapping of the surface composition and stratigraphy of major elements, radioactive elements, and hydrogen at both asteroids. Here, we describe the overall design of the GR/NS and compare the expected performance of the neutron spectrometer subsystem to the neutron spectrometer on Mars Odyssey. We also describe radiation damage studies carried out on CdZnTe detectors, which will be components of the primary gamma-ray spectrometer on Dawn. We conclude that provisions for annealing at moderate temperatures (40°C to 60°C) must be made to ensure that the spectrometer will function optimally over the nine-year mission.**

***Index Terms*—Gamma-ray spectroscopy, planets, neutron spectroscopy, semiconductor device radiation effects.**

I. Introduction

DAWN is a NASA Discovery mission led by the University of California at Los Angeles, which will explore two of the largest main-belt asteroids, 1 Ceres and 4 Vesta. It is thought that the accretion of these protoplanets was interrupted by the formation of Jupiter, shortly after the onset of the condensation of the solar nebula. Thus, Ceres and Vesta contain a record of conditions at the earliest time in our solar system's history and are the remnants of the building blocks that formed the planets [1].

Vesta is highly differentiated by igneous processes and is believed to be the source of howardite, eucrite, and diogenite (HED) meteorites [2]. The HED meteorites provide a record of igneous differentiation occurring early in the history of the solar system. Ceres is likely to be water-rich and undifferentiated, and may have a more primitive, chondritic composition [3]. By determining the composition and structure of these protoplanets, Dawn will provide context for a large number of primitive meteorites in our collection, thus providing a better understanding of processes fundamental to solar system evolution [4].

Dawn will be launched in May 2006 and, using solar electric propulsion, will first travel to Vesta, arriving approximately four years after launch. The spacecraft will cascade downward from an initial reconnaissance altitude to two lower circular mapping orbital altitudes around Vesta. During the mapping phase, which will last eleven months, instruments on board the spacecraft will measure surface elemental abundance and topography, measure the magnetic field, and return high-resolution images of the surface. Early in 2011, Dawn will leave Vesta for Ceres. The cruise to Ceres will last three years, which will be followed by a similar mapping phase that will last for 11 months [4].

The Los Alamos National Laboratory (LANL) is responsible for the gamma-ray and neutron spectrometers (GR/NS) on Dawn. The GR/NS will measure the abundance of major elements, including O, Si, Ti, Al, Fe, Ca, and Mg. Knowledge of the composition of all major rock-forming elements is needed to provide context for meteoritic data and to constrain models of planetary structure and evolution. The gamma-ray spectrometer will also determine the abundance of radioactive elements, including K, U, and Th. The ratio of the volatile element K to the refractory element U provides a measure of the depletion of volatile elements in the source material from which the asteroid was accreted. The neutron spectrometer along with the gamma-ray spectrometer will measure the abundance of H and its stratigraphy. H can be in the form of water or hydrated minerals. Ceres, for example, in addition to having a wet, clay veneer, may have polar caps that consist of water ice.

The GR/NS must meet the science objectives of the Dawn mission, surviving launch and functioning for nine years in the space environment while maintaining ample margins with respect to power consumption, mass, and data telemetry rates. To achieve these goals, the Dawn GR/NS draws on heritage from two recent, successful planetary missions, Lunar Prospector and 2001 Mars Odyssey [5], [6]. The GR/NS builds upon LANL's

Manuscript received December 2, 2002; revised May 12, 2003. This work was supported in part by NASA's Planetary Instrument Definition and Development Program, by the Department of Energy (DOE) Office of Nonproliferation Research and Engineering, and by the DOE's High Altitude and Space Monitoring Program under Contract W-7405-ENG-36.

T. H. Prettyman, W. C. Feldman, F. P. Ameduri, B. L. Barraclough, K. R. Fuller, H. O. Funsten, D. J. Lawrence, G. W. McKinney, S. A. Storms, and R. L. Tokar are with Los Alamos National Laboratory, Los Alamos, NM 87545 USA (e-mail: thp@lanl.gov; wfeldman@lanl.gov; fameduri@lanl.gov; bbarraclough@lanl.gov; kfuller@lanl.gov; hfunsten@lanl.gov; djlawrence@lanl.gov; gwm@lanl.gov; sstorms@lanl.gov; rlt@lanl.gov).

E. W. Cascio is with the Northeast Proton Therapy Center, Massachusetts General Hospital, Boston, MA 02114 USA (e-mail: ecascio@partners.org).

C. T. Russell is with the Institute of Geophysics and Planetary Physics, University of California at Los Angeles (UCLA), Los Angeles CA 90024-1567 USA (e-mail: ctrussell@igpp.ucla.edu).

S. A. Soldner and C. Szeles are with eV Products, Saxonburg, PA 16056 USA (e-mail: ssoldner@ii-vi.com; cszeles@ii-vi.com).

Digital Object Identifier 10.1109/TNS.2003.815156

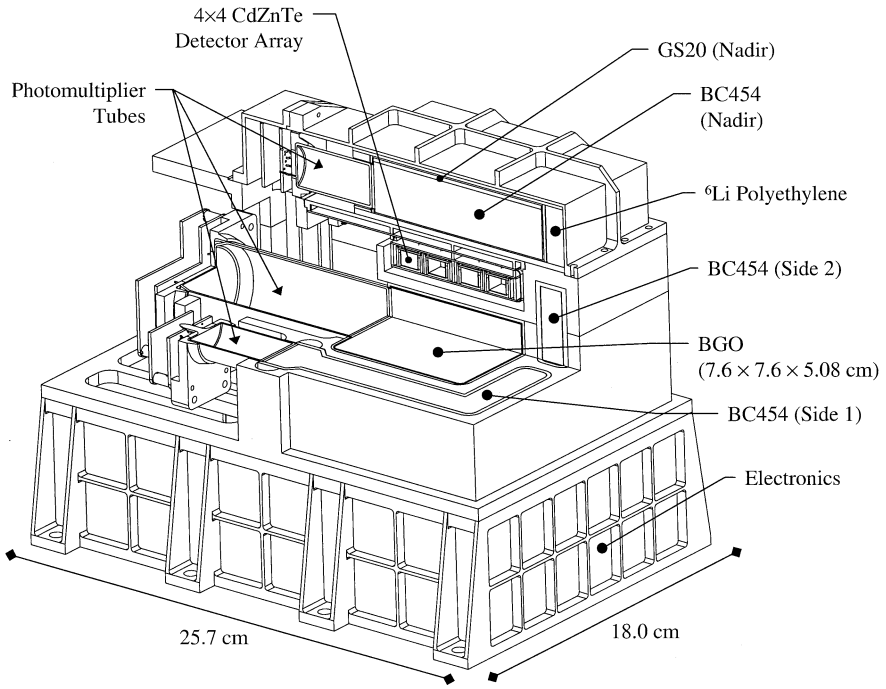

Fig. 1. Cutaway view of the GR/NS for dawn.

expertise in the development of diagnostic instrumentation for the detection of nuclear explosives in and above the Earth's atmosphere, which started with the Vela program in the mid-1960s, extends to the present day, and includes over 330 flight instruments.

In this paper, the design of the GR/NS is presented along with a comparative study of the expected performance of the neutron spectrometer relative to the Mars Odyssey neutron spectrometer. The gamma-ray spectrometer design that will be used for Dawn was described in detail elsewhere. [7]. Here, we present results of a study on the effect of radiation damage on the performance of the CdZnTe component of the gamma-ray spectrometer and engineering measures that will be employed to mitigate the effect of damage during the nine-year mission.

II. Design Overview

The GR/NS will be mounted on the deck of the Dawn spacecraft. Because the instrument will be in close proximity to the bulk of the spacecraft, special provisions have been made in the design of the instrument to allow suppression or subtraction of background radiation originating from the spacecraft. A drawing of the instrument is shown in Fig. 1, and general instrument specifications are given in Table I.

The gamma-ray spectrometer will contain a 4×4 array of coplanar grid CdZnTe semiconductor radiation detectors which will serve as the primary gamma-ray spectrometer. Each element in the array will contain a single $10 \times 10 \times 7.5$ mm CdZnTe crystal and will have pulse-height resolution better than 3% full-width at half-maximum (FWHM) at 662 keV at 20°C. The operating temperature of the GR/NS (20°C) was selected to enable optimal performance of the CdZnTe array. We have observed polarization of CdZnTe detectors at lower temperatures typically used for flight hardware ($-20°C \pm 5°C$).

TABLE I
Instrument Specifications

Specification	Value
Mass	10.5 kg
Power	9.0 W
Dimensions	$25.7 \times 18.0 \times 20.3$ cm^3
Data rate	3.0 kbps
Field of view	2π
Duty cycle on orbit	100%
Operating temperature	20 ± 5°C

Operation at higher temperature also will enable a higher rate of annealing of radiation damage to the CdZnTe crystals during the mission.

Signals from each CdZnTe array element will be digitized on board the spacecraft and sent to ground for analysis. Event mode data from the array elements will be combined to produce a single spectrum, representative of the entire array, with pulse height resolution equal to the average of the individual elements. The array is mounted on top of a BGO crystal that acts as an anticoincidence shield to suppress gamma-rays that come from the spacecraft. The BGO is also used to acquire gamma-ray spectra and will serve to augment the detection efficiency of the CdZnTe array (in coincidence mode) and as a backup, stand-alone, spectrometer if needed. The CdZnTe array has sufficient pulse height resolution and counting efficiency to map all major elements and radioactive elements with improved accuracy compared to the BGO-based spectrometer flown on Lunar Prospector [7].

Surrounding the BGO crystal and CdZnTe array are four boron-loaded plastic scintillators (BC454). The nadir (asteroid) facing and zenith facing elements are primarily sensitive to fast and epithermal neutrons because they are shielded by ^{6}Li-loaded materials that absorb thermal neutrons. The two side facing elements will respond to neutrons of all energies.

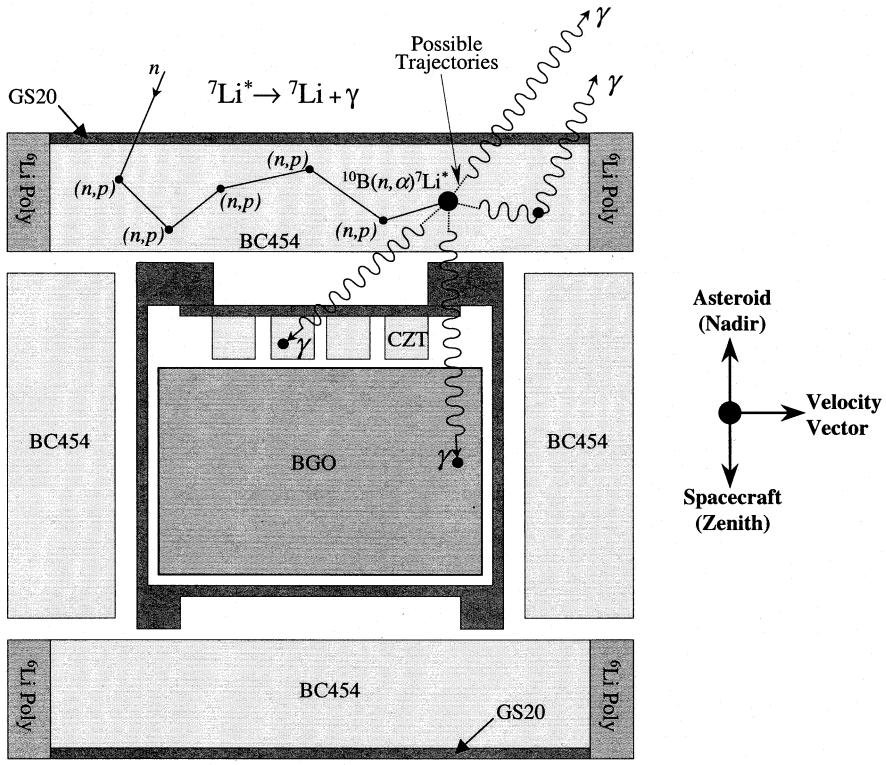

Fig. 2. Cross-sectional view of the GR/NS showing the arrangement of neutron and gamma-ray sensitive elements.

The plastic scintillators are arranged so that the flux of neutrons originating from the spacecraft can be suppressed, separately measured, and subtracted from the neutrons that originate in the asteroid. The plastic scintillators also serve as a cosmic ray suppression system. The use of boron-loaded plastic for planetary spectroscopy was first demonstrated on the Lunar Prospector mission [8]. Light produced in the scintillating components is measured by five photomultiplier tubes (shown in Fig. 1), one for the BGO crystal and four for the BC454 scintillators.

The arrangement of sensors in the GR/NS is shown in Fig. 2 along with a diagram of a fast-neutron interaction with the nadir-facing scintillator. The nadir-facing prism is expected to provide most of the science return because it is well shielded from the spacecraft and is most sensitive to neutrons from the surface of the asteroid. Thermal and epithermal neutrons produce sensible light when they are absorbed via the $^{10}\mathrm{B}(\mathrm{n},\alpha)^7\mathrm{Li}^*$ reaction, which makes 93 keV electron equivalent light output due to the recoil of the reaction products.

Thermal neutrons from the asteroids will be detected by the ^{6}Li-loaded glass (GS20), which is optically coupled to the nadir facing plastic scintillator, forming a phoswhich. Signals from the plastic and glass will be separated and analyzed electronically using a time-domain filter. ^{6}Li-loaded polyethylene surrounds the nadir and zenith facing scintillators in order to provide shielding from thermal neutrons originating from the spacecraft. The thickness of the Li-loaded glass (2 mm) was selected so that the glass would be nearly opaque to thermal neutrons. The thermal neutron count rate will be determined by subtracting a portion of the BC454 count rate, which is sensitive only to epithermal neutrons, from the Li-loaded glass count rate, which is sensitive to both thermal and epithermal neutrons. In order to obtain epithermal and fast neutron detection efficiencies comparable to those achieved by the Mars Odyssey neutron spectrometer, the dimensions of the nadir and zenith facing BC454 components were selected to be $9.87 \times 10.50 \times 2.54$ cm.

Fast neutrons will be separated from epithermal and thermal neutrons by detecting in coincidence the light output from proton recoils produced by interactions between the fast neutron and the plastic followed later in time by light output when the neutron is absorbed at low energy by $^{10}\mathrm{B}$. This characteristic double-pulse signature can be observed for neutrons above 700 keV. The light produced by the prompt interaction of a fast neutron and the hydrogen in the plastic provides a measure of the energy of the incident neutron. This approach for fast neutron spectroscopy for planetary science was demonstrated on Lunar Prospector and Mars Odyssey [8], [9].

The 478 keV gamma-ray produced by the decay of $^7\mathrm{Li}^*$ when detected in coincidence with the 93 keV of sensible light from the $^{10}\mathrm{B}(\mathrm{n},\alpha)$ reaction in the plastic will be used as a calibration line for the gamma-ray sensing elements. Based on count rates observed during the cruise- and mapping-phases of Lunar Prospector and Mars Odyssey, ample gamma-rays are produced by this reaction for calibration during all phases of the mission.

III. Neutron Spectrometer: Expected Performance

The Dawn neutron spectrometer derives much of its heritage from Mars Odyssey, which flew a block of boron-loaded plastic that was segmented into four optically isolated prisms that were viewed by separate photomultipler tubes. A pair of prisms was

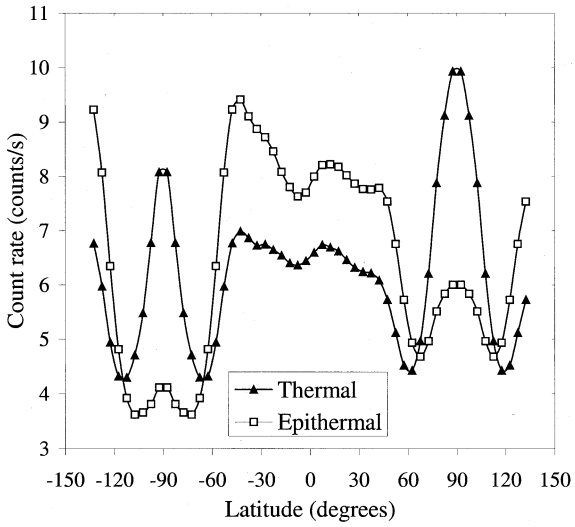

Fig. 3. Longitudinally averaged thermal and epithermal count rates measured by the neutron spectrometer subsystem of the 2001 Mars Odyssey Gamma-Ray Spectrometer. The count rates are mirrored at the poles ($\pm 90°$) and extended to improve visualization of the polar caps. The lines are provided to guide the eye. The count rates shown are averaged over the mapping phase of the mission from February 2002 to November 2002.

oriented on the line of motion of the spacecraft, one facing in the direction of motion and the other facing the opposite direction. The forward facing prism saw an enhanced contribution from thermal neutrons owing to the high speed of the spacecraft (approximately 3.4 km/s) relative to the average speed of thermal neutrons (approximately 1.9 km/s on Mars). Both the forward and backward facing prisms were sensitive to the spacecraft background and epithermal neutrons from the surface of Mars. A count rate that is proportional to the thermal neutron leakage flux can be obtained by subtracting the count rate measured by the backward facing prism from the forward facing prism [10]. Epithermal neutrons were measured by a nadir-facing prism, which was shielded from thermal neutrons by a cadmium foil and partially shielded from the spacecraft by the other three prisms. Because the mass of Ceres and Vesta are small compared to Mars, the orbital speeds (200- to 300 m/s) will be too low to use spacecraft motion to separate thermal and epithermal neutron signatures. This motivated our use of Li-loaded glass for thermal neutron detection on Dawn.

Longitudinally averaged thermal- and epithermal-neutron count rates measured by Mars Odyssey are given in Fig. 3. The counting rate data shown have been averaged over time from late winter to mid-summer in the northern hemisphere. The prominent peaks that occur in the thermal neutron count rate at the poles are caused by the presence of CO_2 in the form of seasonal frost. Both the thermal- and epithermal-count-rates achieve their minimal values in the terrain surrounding the poles (poleward of 50°), which is thought to be rich in water ice present near the surface, buried beneath a thin layer of dry material [11], [12]. Maximum epithermal count rates are achieved equatorward of 50°, where water ice is unstable. Variations in thermal and epithermal count rates in regions where water ice is unstable could be caused by the presence of water in the form of hydrated mineral deposits.

The spatial resolution that can be achieved by an orbiting spectrometer is roughly (to within 30%) 1.5 times the altitude of the spacecraft [13]. So, the footprint of the Mars Odyssey neutron spectrometer was about 600 km FWHM at the surface from an orbital altitude of 400 km, which corresponds to approximately 10° of arc-length (the diameter of Mars is approximately 6800 km). The sensitivity of the spectrometer is sufficient to enable observation of seasonal changes in the thickness and spatial distribution of polar CO_2 frost (on the time scale of two weeks), and to detect minute variations (less than 0.5 weight percent) in water concentration at mid-to-equatorial-latitudes.

The Dawn spacecraft will enter into circular mapping orbits around Vesta and Ceres, with most of the time (130- to 140-days) spent in a 130 km altitude orbit at Vesta and in a 150 km altitude orbit at Ceres. The average diameters of Vesta and Ceres are 516 and 940 km, respectively. Consequently, the neutron spectrometer should be able to resolve surface features separated by greater than 40° of arc length on Vesta and greater than 30° on Ceres. The resolution achieved during mapping will be sufficient to analyze global-scale variations in composition. Higher resolution (approximately 25° on Vesta and 10° on Ceres) will be achieved during a low altitude (75 km) mapping phase, which is expected to last 25 days at each of the asteroids. A factor-of-three improvement in resolution can be achieved if spatial deconvolution methods are applied to the mapping data and if sufficient statistical precision is obtained.

We used a Monte Carlo simulation to estimate thermal and epithermal count-rates measured by the nadir facing sensors while in orbit around Ceres and Vesta. MCNPX was used to simulate the surface output of neutrons for different materials that may be found on the surface of Ceres and Vesta [14]. MCNPX models the interaction of energetic cosmic rays with the surface, the production of fast neutrons and their moderation within and leakage from the surface. A separate Monte Carlo code was developed to model the transport of neutrons from the surface to the spacecraft and their interaction with the neutron sensing elements in the spectrometer. The simulation takes into account the speed of the spacecraft and the gravitational binding of thermal neutrons (important only for the terrestrial and more massive outer planets) and the effect of altitude on count rate.

Simulated count rates are given in Fig. 4 for variable amounts of water in eucrite (which is assumed for the composition of Vesta) measured from orbit at 130 km altitude around Vesta. The points (from top to bottom) shown correspond to 0%, 0.1%, 0.5%, 1%, 2%, 3%, 5%, 10%, and 100% water by weight. The epithermal count rate decreases monotonically with water abundance and is known to be insensitive to composition other than water for common planetary materials.

The uncorrected response, plotted on the x-axis, is the raw count rate that would be observed by the lithiated glass, which is sensitive to both thermal- and epithermal-neutrons. The corrected response was obtained by subtracting $0.58 \times$ the count rate of the boron-loaded plastic from the lithiated glass, which provides a proxy for the thermal neutron count rate. The amount that must be subtracted was determined by comparing the count rate predicted for the lithiated glass to the thermal neutron flux (for neutron energies less than 0.4 eV) for water and dry material.

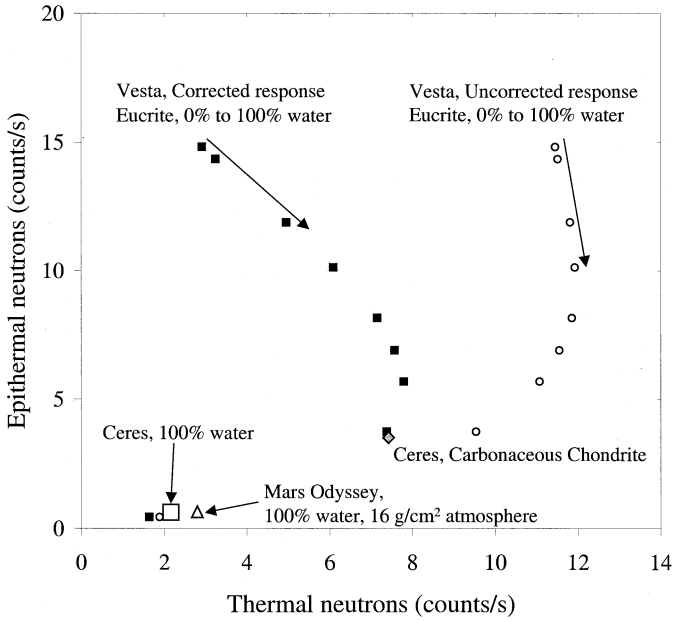

Fig. 4. Comparison of thermal and epithermal count rates for the Mars Odyssey and Dawn neutron spectrometers. All of the data points were calculated using a Monte Carlo code.

Simulated count rates for the Dawn neutron spectrometer for carbonaceous chondrite and 100% water (both of which are possible surface materials on Ceres) from orbit around Ceres at 150 km altitude are shown in Fig. 4. The thermal neutron count rates were corrected to remove the epithermal contribution. For comparison, the count rate that would be measured by the Mars Odyssey neutron spectrometer in orbit around Mars for a terrain consisting of 100% water ice distributed over the entire footprint of the spectrometer is also shown. The simulation shows that the count rates expected for Dawn and those achieved for Mars Odyssey are similar, despite the smaller size of the asteroids. We conclude that Dawn has ample sensitivity to measure the ranges of water abundance and composition expected at Vesta and Ceres.

IV. CdZnTe: Radiation Damage and Annealing

CdZnTe has limited heritage for space applications. Consequently, the BGO scintillator must serve both as a back-shield for the CdZnTe array and as a backup spectrometer in the event that the CdZnTe array fails to function as required. Our chief concern is that the effect of radiation damage on the performance of CdZnTe in the space environment is not well known. Consequently, we have carried out experiments to determine the magnitude of the effect and whether damage can be removed by annealing.

While several future missions will use CdZnTe for various applications, CdZnTe spectrometers have been flown on only one previous mission for which gamma-ray spectroscopic performance was characterized before and after flight. In 1997, on board the Russian space station MIR, six CdZnTe single crystal devices with planar electrodes (each crystal was $10 \times 10 \times 3$ mm, manufactured by eV Products) were used to monitor the diffusion of a radiotracer in a liquid metal diffusion experiment carried out by the University of Alabama, Huntsville [15]. The experiment was in low earth orbit for approximately four months. MIR's orbit traversed the south Atlantic anomaly (SAA), a region where the radiation belts dip close to the Earth. While over the SAA, the CdZnTe detectors witnessed elevated count rates, indicating increased exposure to the terrestrial inner radiation belt energetic particle environment. The pulse height resolution of the detectors was characterized prior to launch and upon return from MIR. No change in the performance of the detectors was observed. [16].

An array of 17 CdZnTe detectors (each crystal was 1.5 mm thick) was flown on a Spanish astrophysics mission (LEGRI/Minisat-01), launched in 1997. The time-variation of the spectral shapes and relative count rates recorded by the detectors was reported in 2001 [17]. Spectral shapes were found to be stable over a two year period in low earth orbit, which suggests that any radiation damage accrued by the detectors produced negligible change in device electronic properties.

Radiation damage studies of CdZnTe have been carried out using accelerator proton sources, and a review of this work is given by Franks, *et al.* [18] They reported that exposure to 200 MeV protons with a fluence of 5×10^9 cm^{-2} (a dose of approximately 0.2 kilorads) caused a factor of two loss in pulse height resolution at 122 keV for a 3 mm thick planar CdZnTe detector. Their study also shows that the magnitude of the effect of radiation damage on performance is device specific. The change in performance at these dose levels is probably associated with increased electron trapping [19], [20], which may account for the variation in the effect of radiation on the performance of different devices following irradiation. It has also been reported that the performance of CdZnTe can be recovered by annealing at room temperature or elevated temperatures [21], [22].

The dose to CdZnTe crystals for the Dawn mission is expected to be 0.2 kilorads/yr [23], [24]. This estimate assumes that the effective thickness of the material surrounding the crystal is 2.7 $\mathrm{g/cm}^2$. The surrounding neutron-sensitive elements in the Dawn GR/NS are at least 3 $\mathrm{g/cm}^2$ thick and are loaded with natural boron and ^{6}Li. Therefore, they will act as an effective shield, minimizing activation by thermal neutrons originating from outside the instrument. Protons incident on the CdZnTe array with energies between 60- and 100-MeV are expected to be the primary source of damage during the mission.

To determine the effect of radiation damage on CdZnTe detectors for Dawn, we irradiated 12 coplanar grid CdZnTe detectors. Engineering test detectors manufactured by eV Products for the Dawn mission were used in the study. Each detector was an operational coplanar grid device with a $10 \times 10 \times 7.5$ mm crystal mounted in a prototype flight assembly. The performance of the detectors was highly variable. However, at least four devices operated near the target flight performance (3% FWHM at 662 keV). The remaining detectors made a peak at 662 keV, but had relatively poor performance and were unsuitable for flight.

Exposure to energetic protons was carried out at the Harvard Cyclotron Laboratory (HCL) in April of 2002. The detectors were exposed to protons with a mean energy of 153.7 MeV in dark conditions and without applied bias. Because the detectors are expected to operate primarily during the mapping phase of

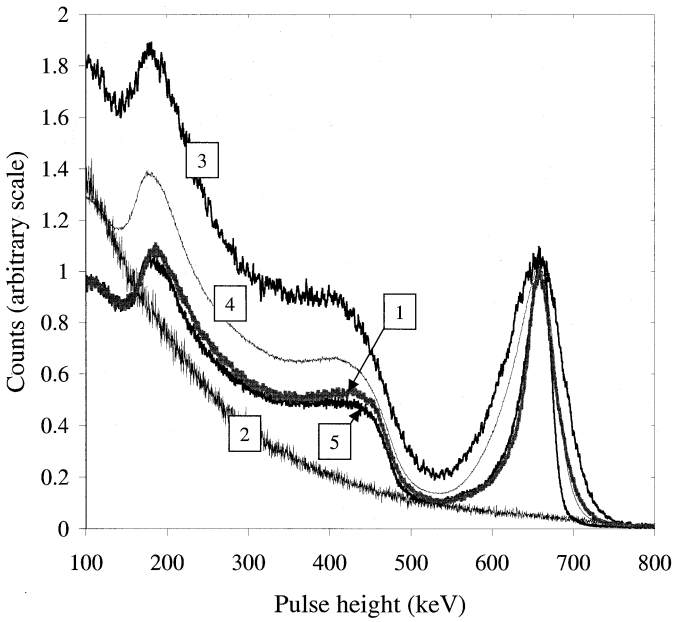

Fig. 5. Spectra acquired for K26–04: (1) prior to irradiation; (2) immediately after irradiation; (3) after annealing for 33 h at 60°C; (4) following three months in storage at room temperature; and (5) after annealing for 24 h at 40°C followed by 24 h at 60°C. Counting rates of all spectra are normalized at the centroid of the full-energy peak.

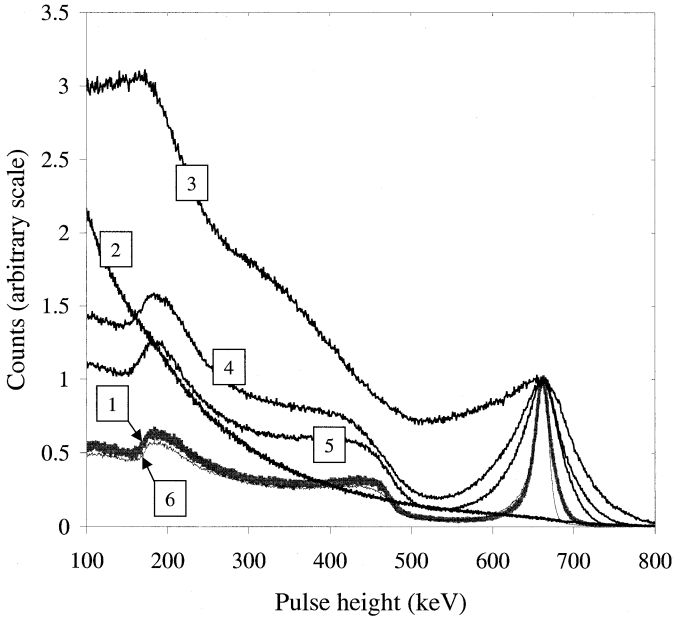

Fig. 6. Spectra acquired for K26–01: (1) prior to irradiation; (2) immediately after irradiation; (3) following three months in storage at room temperature, 22 h at 40°C and 182 h at 60°C; (4) following 115 h at 60°C; (5) following 23 h at 60°C; and (6) following 218 h at 60°C. Counting rates of all spectra are normalized at the centroid of the full-energy peak.

the mission, which is short compared to cruise, we chose not to bias the devices during irradiation and subsequent annealing cycles. During irradiation, the dark current induced by proton interactions was monitored in order to determine the rate at which trapping centers were produced in the crystal. The current was observed to decrease exponentially with an e-fold reduction in magnitude occurring at a fluence of $3 \times 10^{11} \mathrm{cm}^{-2}$.

The detectors were exposed to fluences of 153.7 MeV protons ranging from $1 \times 10^{9} \mathrm{cm}^{-2}$ to $5 \times 10^{10} \mathrm{cm}^{-2}$. Using the TRIM code [25], we estimated that a fluence of $5 \times 10^{10} \mathrm{cm}^{-2}$ at 153.7 MeV will cause as much damage as a dose of 0.6 kilorads by energetic protons encountered during the mission (which will have a mean energy between 60- and 100-MeV at the sensor). Thus, the maximum dose in our experiment corresponds to the dose received over approximately one-third of the mission.

Post-irradiation characterization revealed that detectors exposed to the lowest dose suffered minor losses in pulse height resolution. For example, detector K26–02 had a pulse height resolution of 2.8% FWHM at 662 keV before irradiation. After being exposed to a fluence of $1 \times 10^{9} \mathrm{cm}^{-2}$, the pulse height resolution was 3.4%. The loss in resolution generally increased with dose. Above $5 \times 10^{9} \mathrm{cm}^{-2}$, we were unable to identify a peak at 662 keV for most detectors. Because the dose at which the onset of performance degradation is low compared to the dose expected over the Dawn mission, annealing was investigated as a potential engineering measure to mitigate the effects of radiation damage. Annealing of two detectors is described here.

Detector K26–04 was exposed to a fluence of $5 \times 10^{9} \mathrm{cm}^{-2}$. Spectra acquired for this detector for a $^{137}\mathrm{Cs}$ source (662 keV gamma-rays) before and after irradiation and following annealing are shown in Fig. 5. The spectrum labeled (1) was acquired prior to irradiation. The width of the 662 keV full energy peak was 5.9% FWHM. The spectrum was obtained for a bulk bias of -1000 V and a differential bias of -40 V. The operational parameters of coplanar grid detectors and the effect of bulk bias, differential bias, and differential gain settings on pulse height resolution is described in detail elsewhere [26]. The settings prior to irradiation will be referred to as the nominal settings in the discussion that follows. Following irradiation, bulk bias, differential bias, and differential gain were adjusted over a wide range; however, we were unable to find a full energy peak. A representative post-irradiation spectrum is labeled (2) in Fig. 5.

We then annealed the detector at 60°C for 33 h. Consequently, we were able to identify a peak at the lowest differential gain setting and at nominal bias settings. The spectrum is labeled (3) in Fig. 5. The resolution of the peak improved when we increased bulk bias, which indicated that increased electron trapping was likely the cause of reduced resolution. Next, the detector was placed in storage for three months to determine if significant improvement in performance would occur following annealing at room temperature. The resolution was found to improve considerably. The spectrum measured following this step is labeled (4) in Fig. 5, obtained with nominal bias settings with the differential gain at the minimum setting. Finally, we were able to restore the resolution of the detector to that achieved prior to irradiation with two anneal steps: 24 h at 40°C followed by 24 h at 60°C. The final spectrum, labeled (5) in Fig. 5, was obtained with nominal bias settings and with the differential gain adjusted to achieve the best resolution.

Detector K26–01 was exposed to a fluence of $5 \times 10^{10} \mathrm{cm}^{-2}$, equivalent to roughly one third of the dose expected during the Dawn mission. Prior to irradiation, this detector had a pulse height resolution of 3.5% FWHM, slightly worse than the target performance of the flight detectors for Dawn. A pre-irradiation

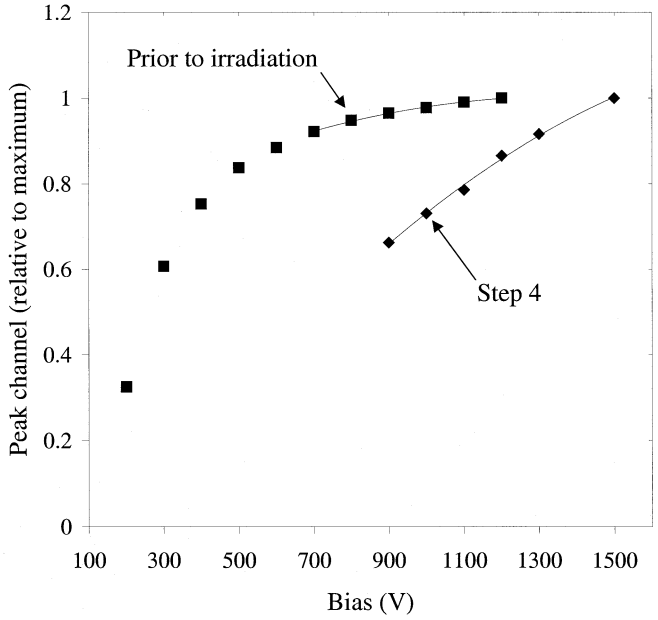

Fig. 7. Peak channel for the 59.5 keV $^{241}\mathrm{Am}$ gamma-ray as a function of bulk bias before irradiation and after step (4) for K26–01.

spectrum is labeled (1) in Fig. 6. Following irradiation, a peak could not be found and a sequence of annealing steps was undertaken that ultimately restored the performance of the detector to its pre-irradiation performance. These steps are outlined in Fig. 6. All of the spectra shown in Fig. 6 were measured with optimal pre-irradiation bias settings (bulk bias of -1200 V and differential bias of -40 V). The differential gain was always set at its minimal value except for the pre-irradiation spectrum (1) and the final spectrum (6). Unlike K26–04, we observed very little change in the post-irradiation spectrum following three months in storage. The total amount of time spent at elevated temperatures was approximately 22 days (22 h at 40°C and 538 h at 60°C).

In order to gain further insight into the cause of reduced pulse height resolution, we measured the peak channel for the 59.5 keV gamma-ray from $^{241}\mathrm{Am}$ as a function of applied bias before irradiation and immediately following step (4). The results of this experiment are shown in Fig. 7. The results of this experiment are shown in . Prior to irradiation, the peak location begins to saturate above 700 V. However, following step (4), the peak location is still increasing at 1500 V. This indicates that the electron mobility-lifetime product is substantially lower in step (4) than before irradiation. This confirms that damage causes a reduction in the electron mobility-lifetime product, which is likely the primary cause of reduced resolution.

V. Conclusion

The Dawn GR/NS was designed to provide an accurate and robust measurement system that fit within the cost and resource constraints of the mission, with ample margins and sufficient heritage to maximize the science return during the nine-year mission to the asteroid belt. Features of the GR/NS include provisions to suppress and subtract spacecraft background and the ability to fully resolve gamma-ray peaks for most elements. The latter is provided by new technology, CdZnTe, which will make its debut in planetary science on the Dawn mission.

The Dawn neutron spectrometer will provide global maps of water-equivalent hydrogen, reveal spatial variations in surface elemental composition on Ceres and Vesta, and provide essential information needed to translate measured gamma-ray counting rates into elemental abundances. Despite the smaller size of the asteroids, neutron count rates predicted for the Dawn GR/NS in mapping orbit around Ceres and Vesta are similar to count rates observed by the Mars Odyssey neutron spectrometer, which have been analyzed to determine global maps of water-equivalent hydrogen and seasonal variations in the thickness and extent of polar CO_2 frost on Mars. The Dawn neutron spectrometer builds on the success of Mars Odyssey, using proven technology (boron-loaded plastic scintillators) to achieve our science objectives. Future work on the neutron spectrometer will involve the development of flight electronics for the Li-glass/BC454 phoswhich time-domain filter.

An array of CdZnTe detectors will serve as the primary gamma-ray spectrometer on Dawn, providing significantly improved pulse height resolution compared to scintillators flown on previous planetary mission. We have shown that the performance of damaged CdZnTe detectors can be restored for doses expected during the Dawn mission by annealing at elevated temperatures. For example, one month of annealing at 60°C may be required for every three years of operation in the space environment. Furthermore, we have found that annealing occurs at operating temperatures (20°C), which may reduce or eliminate the need to anneal at higher temperatures.

This conclusion is further supported by the observation that the CdZnTe detectors flown on MIR showed no significant degradation in performance after four months in low earth orbit, while detectors exposed to equivalent prompt doses of energetic protons at the HCL (for example, K26–04) showed significant degradation. Because the Dawn CdZnTe array elements are significantly thicker than detectors that have been previously flown, they are expected to be more susceptible to changes in electron trapping caused by radiation damage. Consequently, the reduction in resolution due to radiation damage of CdZnTe by energetic particles in the space environment will be mitigated by including a capability for annealing at elevated temperatures on Dawn. Further work will be carried out on the remaining ten damaged detectors to determine optimal strategies for annealing and methods to optimize coplanar grid settings on damaged detectors.

References

[1] J.-C. Liou and R. Malhotra, "Depletion of the outer asteroid belt," *Sci.*, vol. 275, pp. 375–377, Jan. 1997.
[2] R. P. Binzel and S. Xu, "Chips off asteroid-4 vesta: Evidence for the parent body of basaltic achondrite meteorites," *Sci.*, vol. 260, no. 5105, pp. 186–191, Apr. 1993.
[3] D. L. Mitchell *et al.*, "Radar observations of asteroids 1 ceres, 2 pallas, and 4 vesta," *Icarus*, vol. 124, no. 1, pp. 113–133, Nov. 1996.
[4] C. T. Rusell *et al.*, "Dawn discovery mission: A journey to the beginning of the solar system," *Meteoritics Planetary Sci.*, vol. 37, no. 7, p. A123, July 2002.
[5] A. B. Binder, "Lunar prospector: Overview," *Sci.*, vol. 281, pp. 1475–1476, 1998.
[6] J. Bell, "Tip of the Martian Iceberg," *Sci.*, vol. 297, no. 5578, pp. 60–61, July 2002.

[7] T. H. Prettyman, W. C. Feldman, K. R. Fuller, S. A. Storms, S. A. Soldner, C. Szeles, F. P. Ameduri, D. J. Lawrence, M. C. Browne, and C. E. Moss, "CdZnTe gamma-ray spectrometer for orbital planetary missions," *IEEE Trans. Nucl. Sci.*, vol. 49, pp. 1881–1886, Aug. 2002.

[8] W. C. Feldman, B. L. Barraclough, K. R. Fuller, D. J. Lawrence, S. Maurice, M. C. Miller, T. H. Prettyman, and A. B. Binder, "The lunar prospector gamma-ray and neutron spectrometers," *Nucl. Instrum. Methods*, vol. A422, pp. 562–566, 1999.

[9] W. C. Feldman *et al.*, "Fast neutron flux spectrum aboard mars odyssey during cruise," *J. Geophys. Res.*, vol. 107, no. A6, p. 1083, 2002.

[10] W. C. Feldman, D. M. Drake, R. D. O'Dell, F. W. Brinkley Jr., and R. C. Anderson, "Gravitational effects on planetary neutron flux spectra," *J. Geophys. Res.*, vol. 94, no. B1, pp. 513–525, Jan. 1989.

[11] W. C. Feldman *et al.*, "Global distribution of neutrons from mars: Results from mars odyssey," *Sci.*, vol. 297, no. 5578, pp. 75–78, July 2002.

[12] W. V. Boynton *et al.*, "Distribution of hydrogen in the near surface of mars: Evidence for subsurface ice deposits," *Sci.*, vol. 297, no. 5578, pp. 81–85, July 2002.

[13] R. C. Reedy, J. R. Arnold, and J. I. Trombka, "Expected gamma ray emission spectra from the lunar surface as a function of chemical composition," *J. Geophys. Res.*, vol. 78, no. 26, pp. 5847–5866, Sept. 1973.

[14] L. S. Waters, Ed., "MCNPX User's Guide," Los Alamos Nat. Lab., Los Alamos, NM, document LA-UR-99-6058, 1999.

[15] R. M. Banish and L. B. Jalbert, "In-situ diffusivity measurement technique," *Gravitat. Effects Mater. Fluid Sci.*, vol. 24, no. 10, pp. 1311–1320, 1999.

[16] R. M. Banish, private communication, Univ. Alabama, Ctr. Microgravity Mater. Res., Huntsville, AL, Jan. 2002.

[17] V. Reglero, F. Ballesteros, P. Blay, E. Porras, F. Sanchez, and J. Suso, "LEGRI operations. Detectors and detector stability," *Astrophys. Space Sci.*, vol. 276, no. 1, pp. 239–253, 2001.

[18] L. A. Franks *et al.*, "Radiation damage measurements in room-temperature semiconductor radiation detectors," *Nucl. Instrum. Methods*, vol. A428, pp. 95–101, 1999.

[19] L. S. Varnell, W. A. Mahoney, E. L. Jull, and J. F. Butler, "Radiation effects in CdZnTe gamma-ray detectors produced by 199 MeV protons," *Hard X-Ray Gamma-Ray Detector Phys.—Proc. SPIE*, vol. 2806, pp. 424–431, 1996.

[20] K. R. Slavis *et al.*, "Performance of a prototype CdZnTe detector module for hard X-ray astrophysics," in *X-Ray Gamma-Ray Instrum. Astron. XI—Proc. SPIE*, vol. 4140, 2000, pp. 249–256.

[21] L. M. Bartlett *et al.*, "CdZnTe strip detectors for astrophysical arc second imaging and spectroscopy: detector performance and radiation effects," in *Gamma-Ray Cosmic-Ray Detectors, Tech., Missions—Proc. SPIE*, vol. 2806, 1996, pp. 616–628.

[22] L. M. Bartlett *et al.*, "Radiation damage and activation of CdZnTe by intermediate energy neutrons," in *Hard X-Ray/Gamma-Ray Neutron Opt., Sensors, Applicat.—Proc. SPIE*, vol. 2859, 1996, pp. 10–16.

[23] J. Feynman, G. Spitale, J. Wang, and S. Gabriel, "Interplanetary proton fluence model: JPL 1991," *J. Geophys. Res.*, vol. 98, no. A8, pp. 13 281–13 294, 1993.

[24] W. A. Livesey, JPL, Interoffice Memorandum 5052-2001-050, Mar. 28, 2001.

[25] J. F. Ziegler, J. P. Biersack, and U. Littmark, *The Stopping and Range of Ions in Solids*. New York: Pergamon Press, 1985.

[26] M. Amman and P. N. Luke, "Optimization criteria for coplanar grid detectors," *IEEE Trans. Nucl. Sci.*, vol. 46, pp. 205–212, June 1999.